

ELECTRODE PHENOMENA AND PLASMA ACCELERATION

A. N. Babenko, É. P. Kruglyakov,
and V. M. Fedorov

In the experiments described, an organized acceleration of a plasmoid to high velocities ($0.5-2 \cdot 10^8$ cm/sec) was obtained by use of electrodes with a special ribbed surface structure in the accelerator. This paper is a continuation of a series of papers [1-3] on the effect of electrode processes on plasma acceleration in electrode accelerators.

Plasma acceleration was investigated in a rail accelerator with a transverse magnetic field H_z under conditions close to the plane layer configuration. Electrons in the bunch were magnetized ($\omega_H \tau_{ei} \gg 10$). The accelerator geometry is shown in Fig. 1, where 1 is the base of the electrode (stainless steel), 2 is a transverse rib (tantalum), 3 is insulating material (mica, ceramic), 4 is a conducting cylindrical segment (copper), and 5 is a contact tab (tantalum).

The basic data about plasma processes were obtained by noncontact methods:

- 1) recording of the light from the plasmoid was accomplished with electrooptical converters;
- 2) monitoring of the admission of hydrogen, the degree of ionization of the preliminary plasma, and its initial geometry was accomplished with a Michelson optical interferometer with a 140-mm interference field [2, 3].

This same interferometer in conjunction with ruby and neodymium lasers in pulsed and quasicontinuous modes (light sources) and electrooptical converters (recording system) provided a study of the dynamics of plasma acceleration with high time (better than 10^{-8} sec) and spatial ($\ll 1$ mm) resolutions. The method of optical interferometry with the indicated time and spatial resolution made it possible to observe electron concentrations in the plasma as a function of the two spatial coordinates x and y and the time t ,

$$N(x, y, t) = \int n(x, y, z, t) dz$$

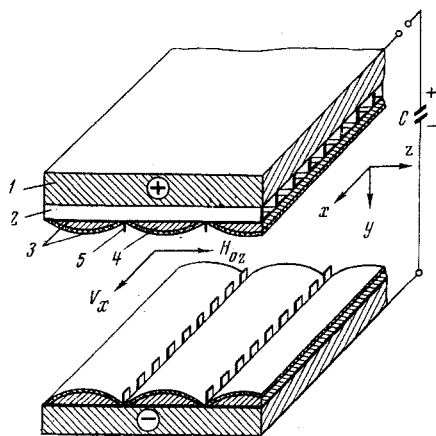


Fig. 1

For better approximation to a plane-layer model, a special system of pulsed gas input was used (electrodynamic valves with a flow-spreading chamber) which made it possible to obtain in the interelectrode gap a gas cloud having the dimensions $\Delta x \approx 2.5$ cm, $\Delta y = 3$ cm, and $\Delta z \sim 10$ cm.

In typical injector operating modes, the hydrogen concentration in the "gas parallelepiped" was $n_{H_2} \approx 5 \cdot 10^{15}$ cm $^{-3}$ for a total number of injected molecules $N_0 \approx 3 \cdot 10^{17}$. The magnitude of the nonuniformity in gas distribution across the gap was no more than 10% [2]. Preliminary ionization was accomplished in a transverse magnetic field $H_{0z} = 7$ kG by a low-capacity oscillating discharge ($0.1 \mu F \times 25$ kV, $T = 1.2 \mu sec$). At the time the accelerating bank ($C = 18 \mu F$, $U = 20-30$ kV, $T/4 = 3 \mu sec$) was turned on, the degree of ionization α at the center of the gap was approximately 50% and fell to 10% at the electrodes.

Novosibirsk. Translated from Zhurnal Prikladnoi Mekhaniki i Tekhnicheskoi Fiziki, No. 3, pp. 140-144, May-June, 1971. Original article submitted October 29, 1970.

© 1973 Consultants Bureau, a division of Plenum Publishing Corporation, 227 West 17th Street, New York, N. Y. 10011. All rights reserved. This article cannot be reproduced for any purpose whatsoever without permission of the publisher. A copy of this article is available from the publisher for \$15.00.

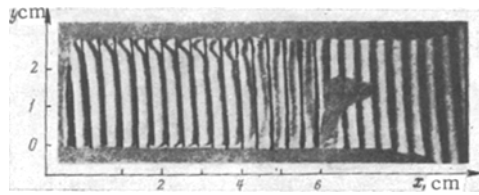


Fig. 2

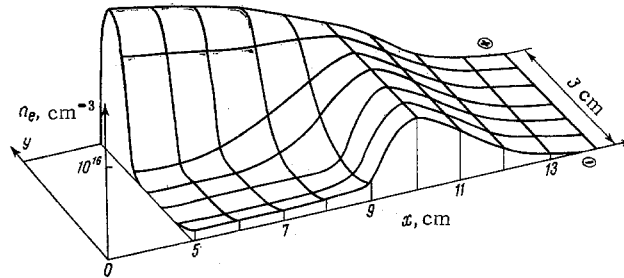


Fig. 3

According to estimates, the mean free path for neutral atoms in such a plasma was $\lambda_H \approx 2$ mm; for protons it was $\lambda_H \approx 0.3$ mm. The magnetization parameter for ions was $\omega_{H_i} \tau_{ii} < 1$ and for electrons, $\omega_{H_e} \tau_{ei} \sim 10$. As is clear from these estimates, the particle mean free path was considerably less than the dimensions of the plasma layer, which permitted complete capture of the gas in acceleration.

The electrode system of the rail accelerator was located in a vacuum space pumped down through a nitrogen trap by an oil-vapor pump to $1.5 \cdot 10^{-6}$ torr and 10^{-6} torr by using an internal loop cooled by liquid nitrogen. Electrodes of three different configurations were used in the study of acceleration. The plasmoid acceleration time was $\sim 1 \cdot 10^{-6}$ sec in each case. Discussed below are the phenomena observed and the structural features of the electrodes which made it possible to obtain monoenergetic plasmoids at the accelerator exit with velocities above 10^8 cm/sec.

1. Model with Smooth Electrodes. In this case, smooth acceleration to a velocity $v \sim 2 \cdot 10^7$ m/sec over a distance of 6 cm is observed for a plasmoid having a density $n_e \sim 10^{16}$ cm $^{-3}$. (The final velocity of the main mass of ionized gas in coaxial accelerators is approximately the same [4, 5].)

A strong plasma trail associated with outgassing from the electrode is observed outside the current layer at the cathode surface. The electron density increases monotonically toward the cathode varying from 10^{16} to $\approx 10^{17}$ cm $^{-3}$ in a distance of ~ 1 mm at the surface of the electrode. The anode trail has a different structure; an interferogram frame of a plasmoid 10^{-6} sec after the beginning of acceleration is shown in Fig. 2 for the smooth electrode case. The maximum electron density is several millimeters removed from the anode and moves toward the electrode at a velocity of $\sim 10^6$ cm/sec.

Further acceleration (for $\Delta x > 6$ cm) is extremely unstable; the current layer begins to separate from the anode. Attempts at separation are accompanied by potential spikes at the electrodes and the acceleration of small portions of the primary plasma to velocities of the order of 10^8 cm/sec. (Typical magnitude of the velocity of a high-speed rarefied plasma observed ahead of the main bunch in coaxial accelerators and called a forebunch [5].) In this case, the emission of strong plasma jets from the electrodes is observed; they move into the gap with velocities up to 10^7 cm/sec.

The observed anomalies in plasma density distribution in the anode layer are primarily associated with the development of the Hall effect. The essence of this phenomenon, well known to specialists in MHD generators, is the following. In a plasma accelerated across a magnetic field, there arises a longitudinal electric field

$$\vec{E}_x = \frac{m_i}{e} \frac{dv_x}{dt}$$

directed along the line of ion acceleration.

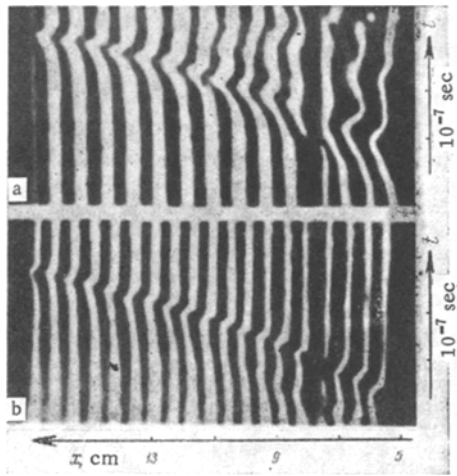


Fig. 4

Upon contact of the polarized plasma with the conducting electrodes, longitudinal electric currents j_x arise in it. The interaction of the latter with the magnetic field H_z leads to plasma acceleration across the channel with the acceleration being directed so that the plasma layer tends to separate from the anode. Split electrodes are used in stationary systems in order to reduce this effect [6]. This method is inapplicable in pulsed accelerators because of the difficulties associated with the problem of rapid switching of current between sections as a consequence of the displacement of the current layer along the electrodes. Nevertheless, the problem of the creation of a longitudinal field E_x can be solved at least for the anode, which is mainly responsible for the "cutoff" of plasma layer acceleration.

Perpendicular to the anode surface, we set up thin conducting plates having a height $h_y(x)$ and oriented along the z axis with a spacing Δx in the direction of acceleration (Fig. 1). With displacement of the current layer between ribs, there now arises an electric field

$$E_x^a = -\frac{h_y(x)}{c} \frac{dH_z}{dt} = -h_y(x) \frac{v_x}{c} \frac{\partial H_z}{\partial x}$$

By selecting the rib height $h_y(x)$, one can equalize the field E_x^a at the anode and the field E_x in the plasma [3].

As far as the cathode is concerned, one can look for means to reduce the area of current contact between plasmoid and cathode [3]. The practicality of this assertion is confirmed by the following considerations. It is well known that in areas of current contact between plasma and cathode (arc spots), the current density reaches values of 10^6 - 10^9 A/cm² [7]. There consequently occurs strong outgassing from the surface of the electrode with the result that plasma density at the cathode is considerably greater than in the interelectrode gap. A sharp increase in plasma density at the cathode with an average gradient $\langle dn_e/dy \rangle \approx 10^{18}$ cm⁻³/cm was actually observed in the experiments described above (Model 1). It is natural that the cathode plasma lag behind the motion of the current layer in the gap during acceleration.

2. Model with Shaped Electrodes. In the experiments described below, the longitudinal field E_x at the anode was created by a system of transverse tantalum ribs oriented along the z axis. Rib height was 10 mm in the region of gas input and decreased monotonically to 2 mm at the exit from the electrodes. The spacing between neighboring sections was 5 mm.

To reduce the area of plasma current contact with the cathode, six longitudinal (along the x axis) ribs 8 mm high at a spacing of 2 cm were installed on the surface of the cathode.

Figure 3 shows the "instantaneous" electron density distribution 10^{-6} sec after the beginning of acceleration for electrodes shaped by the method described. It should be noted that the average plasma density near the cathode is now little different from the density in the interelectrode gap. The cathode trail has practically disappeared. The structure of the anode trail is changed; the electron density rises monotonically toward the anode, now reaching a value $\langle n_{e\max} \rangle \sim 1.5 \cdot 10^{16}$ cm⁻³ in comparison with $n_e \sim 10^{17}$ cm⁻³ for Model 1. The profile of the anode trail shows that its formation is mainly associated with bombardment of the transverse anode ribs by the flow of accelerated plasma. The stable velocity for macroscopic acceleration of the plasma layer as a whole reached $v \sim 4 \cdot 10^7$ cm/sec for Model 2 with the total number of accelerated protons $N_i \sim 2 \cdot 10^{17}$. Thus the creation of a longitudinal electric field at the anode and reduction of the current contact area between plasma and electrode made it possible to obtain higher values for stable plasmoid velocities in comparison with the results obtained in an accelerator with smooth electrodes.

Further improvement of the rail accelerator naturally proceeded in the direction of maximum possible isolation of the plasma from the electrodes. We now turn to a consideration of the last model.

3. Model with Small Plasma-Electrode Contact Area. In the last model, thin contact tabs oriented along the x axis and forming six rows with a 2-cm spacing were mounted on the cathode in place of the six continuous longitudinal tantalum ribs (along the x axis). The flat portions of the cathode between the rows

of tabs were covered by copper bars ($20 \times 2 \text{ cm}^2$) in the shape of segments 3 mm high. These were insulated from the cathode by mica inserts and were covered with ceramic segments on the plasma side (Fig. 1).

A similar construction was employed at the anode with the exception that the contact tabs were mounted on the rib structure described in Model 2 and not on the electrode base. Because of the presence of the copper segments, the previously uniform magnetic field was now corrugated near the electrode surfaces with the maximum field being achieved above the vertices of the segments. Such a field configuration hinders plasma diffusion to the walls.

Figure 4 shows a time-smear interferogram of plasma acceleration (the slit is along the direction of acceleration; in *a* the slit is at the anode and in *b* the slit is at the center of the gap); from these interferograms, one can follow the general trends in the variation of the average electron density $N(x, y, t)$ in a plasmoid as it is accelerated. Analysis of the interferograms reveals the following:

- 1) the longitudinal dimension of the accelerated bunch remains practically unchanged over the entire acceleration cycle;
- 2) the path length over which stable acceleration is achieved increased to 17 cm; in this case, a mass velocity of approximately 10^8 cm/sec was achieved for the plasmoid. Note that in overaccelerated modes and with smaller gas input, plasmoid velocity at the accelerator exit was $\approx 2 \cdot 10^8$ cm/sec;
- 3) the anode trail disappeared almost completely in the final stages of acceleration;
- 4) approximately half the plasma particles were lost in the final stages of acceleration. Thus the number of accelerated protons was $3 \cdot 10^{17}$ and their velocity, 10^8 cm/sec. The kinetic energy of the plasmoid could be estimated from that. It was approximately 250 J.

LITERATURE CITED

1. V. M. Fedorov, "Investigation of rail acceleration of plasma across a magnetic field," *Magnitn. Gidrodinam.*, **1**, No. 2 (1965).
2. É. P. Kruglyakov, V. K. Malinovskii, and V. M. Fedorov, "Investigation of plasma acceleration in rail accelerators," in: *Phenomena in Ionized Gases*, Vol. 3, Gradevinska Knjiga, Beograd (1966).
3. A. N. Babenko, É. P. Kruglyakov, V. V. Kuznetsov, and V. M. Fedorov, "On some peculiarities in electric discharge development in hydrogen across a magnetic field," *Proc. 8th Internat. Conf. on Phenomena in Ionized Gases*, Vienna, 1967, Internat. Atomic Energy Agency, Vienna (1968).
4. J. Marshall, "Performance of hydromagnetic plasma gun," *Phys. Fluids*, **3**, No. 1 (1960).
5. S. Yu. Luk'yanov, I. M. Podgornyi, and S. A. Chuvatin, "Investigation of electrodynamic acceleration of plasmoids," *Zh. Tekh. Fiz.*, **31**, No. 9, 1026 (1961).
6. H. Hurwitz, R. W. Kilb, and G. W. Sutton, "Influence of tensor conductivity on current distribution in a MHD generator," *J. Appl. Phys.*, **32**, No. 2, 205 (1961).
7. J. L. Craston, R. Hancox, A. E. Robson, S. Kaufman, N. T. Miles, A. A. Ware, and J. A. Wesson, "The role of materials in controlled thermonuclear research," *Proc. 2nd U.N. Internat. Conf. on Peaceful Uses of Atomic Energy*, Geneva, Vol. 32, No. 34 (1958), pp. 414-426.